

Ca₉La(PO₄)₇:Eu²⁺,Mn²⁺: an emission-tunable phosphor through efficient energy transfer for white light-emitting diodes

Chien-Hao Huang and Teng-Ming Chen*

Phosphors Research Laboratory and Department of Applied Chemistry,
National Chiao Tung University, Hsinchu 30010 Taiwan

*tmchen@mail.nctu.edu.tw

Abstract: We have synthesized a series of single-composition emission-tunable Ca₉La(PO₄)₇:Eu²⁺,Mn²⁺ (CLP:Eu²⁺,Mn²⁺) phosphors by solid state reactions. Through an effective resonance-type energy transfer, the CLP:Eu²⁺,Mn²⁺ phosphors exhibit a systematically varied hues from green, yellow, and eventually to red and the relative intensity of green and red emissions can be tuned by adjusting the concentration of Mn²⁺, respectively. The energy transfer from Eu²⁺ to Mn²⁺ in CLP:Eu²⁺,Mn²⁺ has been studied and demonstrated to be a resonant type via a dipole-quadrupole mechanism based on the decay lifetime data and the energy transfer critical distance was estimated to be 11.36 Å by using the spectral overlap methods. A warm white light emitting diode (WLED) with CIE chromaticity coordinates of (0.35, 0.31), superior color-rendering index (*Ra*) of 91.5 and lower correlated color temperature (CCT) of 4,496 K was fabricated by combining a 365 nm UV-InGaN chip and a phosphor blend of yellow-emitting (Ca_{0.98}Eu_{0.005}Mn_{0.015})₉La(PO₄)₇ and blue-emitting BaMgAl₁₀O₁₇:Eu²⁺.

©2010 Optical Society of America

OCIS codes: (000.2700) General science.

References and links

1. H. S. Jang, Y. H. Won, and D. Y. Jeon, "Improvement of electroluminescent property of blue LED coated with highly luminescent yellow-emitting phosphors," *Appl. Phys. B* **95**(4), 715–720 (2009).
2. A. A. Setlur, W. J. Heward, Y. Gao, A. M. Srivastava, R. G. Chandran, and M. V. Shankar, "Crystal chemistry and luminescence of Ce³⁺-doped Lu₂CaMg₂(Si,Ge)₃O₁₂ and its use in LED based lighting," *Chem. Mater.* **18**(14), 3314–3322 (2006).
3. M. Batentschuk, A. Osvet, G. Schierming, A. Klier, J. Schneider, and A. Winnacker, "Simultaneous excitation of Ce³⁺ and Eu³⁺ ions in Tb₃Al₅O₁₂," *Radiat. Meas.* **38**(4-6), 539–543 (2004).
4. Z. Hao, J. Zhang, X. Zhang, X. Sun, Y. Luo, S. Lu, and X.- Wang, "White light emitting diode by using α-Ca₂P₂O₇:Eu²⁺, Mn²⁺ phosphor," *Appl. Phys. Lett.* **90**(26), 261113 (2007).
5. J. S. Kim, P. E. Jeon, Y. H. Park, J. C. Choi, H. L. Park, G. C. Kim, and T. W. Kim, "White-light generation through ultraviolet-emitting diode and white-emitting phosphor," *Appl. Phys. Lett.* **85**(17), 3696 (2004).
6. W. J. Yang, and T. M. Chen, "Ce³⁺/Eu²⁺ codoped Ba₂ZnS₃: a blue radiation-converting phosphor for white light-emitting diodes," *Appl. Phys. Lett.* **90**(17), 171908 (2007).
7. C. K. Chang, and T. M. Chen, "White light generation under violet-blue excitation from tunable green-to-red emitting Ca₂MgSi₂O₇:Eu,Mn through energy transfer," *Appl. Phys. Lett.* **90**(16), 161901 (2007).
8. G. Q. Yao, J. H. Lin, L. Zhang, G. X. Lu, M. L. Gong, and M. Z. Su, "Luminescent properties of BaMg₂Si₂O₇:Eu²⁺,Mn²⁺," *J. Mater. Chem.* **8**(3), 585–588 (1998).
9. W. J. Yang, L. Luo, T. M. Chen, and N. S. Wang, "Luminescence and energy transfer of Eu- and Mn-coactivated CaAl₂Si₂O₈ as a potential phosphor for white-Light UVLED," *Chem. Mater.* **17**(15), 3883–3888 (2005).
10. W. J. Yang, and T. M. Chen, "White-light generation and energy transfer in SrZn₂(PO₄)₂:Eu,Mn phosphor for ultraviolet light-emitting diodes," *Appl. Phys. Lett.* **88**(10), 101903 (2006).
11. C. Guo, L. Luan, X. Ding, and D. Huang, "Luminescent properties of SrMg₂(PO₄)₂:Eu²⁺,and Mn²⁺ as a potential phosphor for ultraviolet light-emitting diodes," *Appl. Phys., A Mater. Sci. Process.* **91**(2), 327–331 (2008).
12. W. R. Liu, Y. C. Chiu, Y. T. Yeh, S. M. Jang, and T. M. Chen, "Luminescence and energy transfer mechanism in Ca₁₀K(PO₄)₇:Eu²⁺, Mn²⁺ phosphor," *J. Electrochem. Soc.* **156**(7), J165 (2009).
13. Z. Hao, J. Zhang, X. Zhang, S. Lu, Y. Luo, X. Ren, and X. Wang, "Phase dependent photoluminescence and energy transfer in Ca₂P₂O₇:Eu²⁺, Mn²⁺ phosphors for white LEDs," *J. Lumin.* **128**, 941 (2008).
14. S. Ye, Z. S. Liu, J. G. Wang, and X. P. Jing, "Luminescent properties of Sr₂P₂O₇:Eu,Mn phosphor under near UV excitation," *Mater. Res. Bull.* **43**(5), 1057–1065 (2008).

15. S. Ye, X. M. Wang, and X. P. Jing, "Energy transfer among Ce^{3+} , Eu^{2+} , and Mn^{2+} in $CaSiO_3$," J. Electrochem. Soc. **155**(6), J143 (2008).
16. JCPDS No. 46-0402.
17. V. A. Morozov, A. A. Belik, S. Yu. Stefanovich, V. V. Grebenev, O. I. Lebedev, G. Van Tendeloo, and B. I. Lazoryak, "High-temperature phase transition in the whitlockite-type phosphate $Ca_9In(PO_4)_7$," J. Solid State Chem. **165**(2), 278–288 (2002).
18. J. M. Robertson, M. W. van Tol, W. H. Smits, and J. P. H. Heyene, "Colourshift of the Ce^{3+} emission in monocrystalline epitaxially grown garnet layers," Philips J. Res. **36**, 15 (1981).
19. H. S. Jang, W. B. Im, D. C. Lee, D. Y. Jeon, and S. S. Kim, "Enhancement of red spectral emission intensity of $Y_3Al_5O_{12}:Ce^{3+}$ phosphor via Pr co-doping, and Tb substitution for the application to white LEDs," J. Lumin. **126**(2), 371–377 (2007).
20. P. D. Rack, and P. H. Holloway, "The structure, device physics, and material properties of thin film electroluminescent displays," Mater. Sci. Eng. Rep. **21**(4), 171–219 (1998).
21. R. V. S. S. N. Ravikumar, K. Ikeda, A. V. Chandrasekhar, Y. P. Reddy, P. S. Rao, and J. Yamauchi, "Site symmetry of Mn(II) and Co(II) in zinc phosphate glass," J. Phys. Chem. Solids **64**(12), 2433–2436 (2003).
22. C. C. Chiang, M. S. Tsai, and M. H. Hon, "Synthesis and photoluminescent properties of Ce^{3+} doped terbium aluminum garnet phosphors," J. Alloy. Comp. **431**(1-2), 298–302 (2007).
23. R. Pang, C. Li, L. Shi, and Q. Su, "A novel blue-emitting long-lasting propphosphate phosphor $Sr_2P_2O_7:Eu^{2+},Y^{3+}$," J. Phys. Chem. Solids **70**(2), 303–306 (2009).
24. S. Buddhudu, M. Morita, S. Murakami, and D. Rau, "Temperature-dependent luminescent and energy transfer in europium and rare earth codoped nanostructured xerogel and sol-gel silica glasses," J. Lumin. **83–84**(1-3), 199–203 (1999).
25. N. Ruelle, M. P. Thi, and C. Fouassier, "Cathodoluminescent properties and energy transfer in red calcium sulfide phosphors ($CaS:Eu,Mn$)," Jpn. J. Appl. Phys. **31**(Part 1, No. 9A), 2786–2790 (1992).
26. P. I. Paulose, G. Jose, V. Thomas, N. V. Unnikrishnan, and M. K. R. Warrier, "Sensitized fluorescence of Ce^{3+}/Mn^{2+} system in phosphate glass," J. Phys. Chem. Solids **64**(5), 841–846 (2003).
27. H. Jiao, F. Liao, S. Tian, and X. J. Jing, "Luminescent properties of Eu^{3+} and Tb^{3+} activated $Zn_3Ta_2O_8$," J. Electrochem. Soc. **150**(9), H220 (2003).
28. Y. Tan, and C. Shi, " $Ce^{3+} \rightarrow Eu^{2+}$ energy transfer in $BaLiF_3$ phosphor," J. Phys. Chem. Solids **60**(11), 1805–1810 (1999).
29. G. Blasse, "Energy transfer in oxidic phosphors," Philips Res. Rep. **24**, 131 (1969).
30. D. L. Dexter, "A theory of sensitized luminescence in solids," J. Chem. Phys. **21**(5), 836 (1953).

1. Introduction

In recent years, white light-emitting diodes (white-LEDs) have attracted much attention, in which white light can be generated by a blue-emitting InGaN chip and yellow-emitting phosphor $Y_3Al_5O_{12}:Ce^{3+}$ garnet (YAG: Ce^{3+}). However, the disadvantages of this method are low color-rendering index (CRI, $Ra = 75$) and high color temperature (CCT = 7756 K) [1], due to the lack of red spectral contribution [2,3]. During the past few years, the white LEDs fabricated using (a) near ultraviolet (n-UV) LED or ultraviolet (UV) LED (350–420 nm) coupled with red, green, and blue phosphors [4–6], (b) n-UV LED (380–420 nm) pumped with a single composition green-to-red emission-tunable [7,8] and blue phosphor to improve the Ra and CCT. From this point of view, single-composition yellow-emitting (green of Eu^{2+} and red of Mn^{2+}) phosphors for UV or n-UV excitations have drawn much attentions for solid state lighting. As compared to the InGaN-based blue LED chip combined with YAG: Ce^{3+} phosphor, a white-LED fabricated using a phosphor blend of single-composition emission-tunable phosphor and blue phosphor pumped with UV/NUV chips has advantages of a great Ra , tunable CCT and Commission International de l'Eclairage (CIE) chromaticity coordinates. One of the strategies for generating single-phased emission-tunable phosphor is by co-doping sensitizer and activator into the same host, which is based on the mechanism of energy transfer from sensitizer to activator. The phosphors with energy transfer mechanism of sensitizer/activator, such as Eu^{2+}/Mn^{2+} , have been synthesized and investigated in many hosts. For instance, $Ca_2MgSi_2O_7:Eu^{2+},Mn^{2+}$ [7], $BaMg_2Si_2O_7:Eu^{2+},Mn^{2+}$ [8], $CaAl_2Si_2O_8:Eu^{2+},Mn^{2+}$ [9], $SrZn_2(PO_4)_2:Eu^{2+},Mn^{2+}$ [10], $SrMg_2(PO_4)_2:Eu^{2+},Mn^{2+}$ [11], $KCa_{10}(PO_4)_7:Eu^{2+},Mn^{2+}$ [12], $Ca_2P_2O_7:Eu^{2+},Mn^{2+}$ [13], $Sr_2P_2O_7:Eu^{2+},Mn^{2+}$ [14], $CaSiO_3:Ce^{3+},Eu^{2+},Mn^{2+}$ [15]. To the best of our knowledge, the crystal structure, luminescence properties and energy transfer of Eu^{2+}/Mn^{2+} in $Ca_9La(PO_4)_7$ host have not been reported. We have firstly demonstrated a single-composition green-to-red emission-tunable $Ca_9La(PO_4)_7:Eu^{2+},Mn^{2+}$ phosphor by energy transfer mechanism between the luminescence centers Eu^{2+} and Mn^{2+} , the color can be tuned from green to yellow even to red. We have also proven that a warm white light can be

achieved by increasing the dopant contents of Mn^{2+} . The $\text{Ca}_9\text{La}(\text{PO}_4)_7:\text{Eu}^{2+},\text{Mn}^{2+}$ phosphor exhibits great potential for use in white UV-LED applications to serve as a single-phased phosphor that can be pumped with near-UV or UV-LEDs.

2. Experimental

The $\text{CLP}:\text{Eu}^{2+},\text{Mn}^{2+}$ phosphors were prepared from stoichiometric starting materials of CaCO_3 (A.R. 99.9%), Y_2O_3 (A.R. 99.9%), La_2O_3 (A.R. 99.99%), $(\text{NH}_4)_2\text{HPO}_4$ (Merck $\geq 99\%$), Eu_2O_3 (A.R. 99.99%), and MnO (A.R. 99.9%). The reactant mixture was first pressed into pellets and calcined at 1,473K for 8 h under ambient atmosphere. The obtained samples were further reduced at 1,273K for 8 h under a reducing atmosphere of 15% H_2 /85% N_2 in an alumina boat. The samples were characterized using powder X-ray diffraction (XRD), photoluminescence (PL) and PL excitation (PLE) spectra, decay lifetime, and CIE chromaticity, as described in our previous work [6,7]. The phase purity of $\text{CLP}:\text{Eu}^{2+},\text{Mn}^{2+}$ phosphors was checked by using powder XRD analysis with a Bruker AXS D8 advanced automatic diffractometer with $\text{Cu K}\alpha$ radiation. The measurements of PL and PLE spectra were performed by using a Spex Fluorolog-3 Spectrofluorometer (Instruments S.A., N.J., U.S.A) equipped with a 450W Xe light source and double excitation monochromators. The powder samples were compacted and excited under a 45° incidence angle and the emitted fluorescence was detected by a Hamamatsu Photonics R928 type photomultiplier perpendicular to the excitation beam. Time-resolved measurements were performed with a tunable nanosecond optical-parametric-oscillator/Q-switch-pumped $\text{YAG}:\text{Nd}^{3+}$ laser system (NT341/1/UV, Ekspla). Emission transients were collected with a nanochromator (SpectraPro-300i, ARC), detected with photomultiplier tube (R928HA, Hamamatsu), connected to a digital oscilloscope (LT372, LeCrop) and transferred to a computer for kinetics analysis.

White LED lamps were fabricated by integrating a mixture of transparent silicon resin and phosphors blend of $\text{Ca}_9\text{La}(\text{PO}_4)_7:0.005\text{Eu}^{2+},0.015\text{Mn}^{2+}$ and $\text{BaMgAl}_{10}\text{O}_{17}:\text{Eu}^{2+}$ commodity on an UV-chip (AOT Product No: DC0004CAA, Spec: 370U02C, wavelength peak: 365 ~370 \pm 0.6 nm, chip size: 40x40 mil, forward voltage: 3.8 ~4.0 \pm 0.02 V, power: 10-20 \pm 0.21 mW). The Commission International de l'Eclairage (CIE) chromaticity coordinates for all samples were measured by a Laiko DT-101 color analyzer equipped with a CCD detector (Laiko Co., Tokyo, Japan).

3. Results and discussion

All powder XRD patterns of $\text{Ca}_9\text{Y}(\text{PO}_4)_7$ (CYP) and $\text{CLP}:\text{Eu}^{2+},\text{Mn}^{2+}$ phosphors are shown in Fig. 1. All phases purity of the as-prepared phosphors was analyzed with JCPDS No. 46-0402 [16] as a reference, indicating that the doped Eu^{2+} ions or co-doped $\text{Eu}^{2+}/\text{Mn}^{2+}$ ions have not caused any observable change in the CLP host structure. The compound $\text{Ca}_9\text{La}(\text{PO}_4)_7$ is isostructural to the $\text{Ca}_9\text{Y}(\text{PO}_4)_7$ [16] and $\beta\text{-Ca}_9\text{In}(\text{PO}_4)_7$ [17], $\text{Ca}_9\text{Y}(\text{PO}_4)_7$ has a rhombohedral crystal structure with a space group of $R\bar{3}c$ (No.161), and their lattice parameters are $a = 10.4442\text{\AA}$, $c = 37.324\text{\AA}$, $V = 3525.89\text{ nm}^3$, $Z = 6$ and Ca^{2+} , Y^{3+} (La^{3+}) and P^{5+} ions are have three, one and three crystallographic sites, respectively. The coordination environment of the cations is such that Ca(1) and Ca(2) are eight-coordinated, Ca(3) is nine-coordinated, Y (La) is six-coordinated and P(1), P(2), and P(3) are four-coordinated to oxygen atoms. The ionic radii for eight- and nine-coordinated Eu^{2+} are 1.25 and 1.3 \AA , respectively, and that for eight-coordinated Mn^{2+} is 0.96 \AA ; however, the ionic radii for eight- and nine-coordinated Ca^{2+} cations are 1.12 and 1.18 \AA , respectively. Therefore, based on comparison of the effective ionic radii of cations with different coordination numbers, we have proposed that Eu^{2+} and Mn^{2+} are expected to randomly occupy the Ca^{2+} sites in the host structure.

The concentration dependence of relative PLE and PL intensity of CLP: $x\text{Eu}^{2+}$ ($x = 0.001 \sim 0.1$) under 365 nm excitation was shown in Fig. 3. The PL spectra exhibited a broad band green emission centered at 502 nm, which was imputed to the $4f^65d^1 \rightarrow 4f^7$ of the Eu^{2+} ion. The optimal Eu^{2+} dopant content was found to be 0.005 mole and the PL/PLE intensity was observed to increase with increasing x when $x < 0.005$. For samples with Eu^{2+} dopant content higher than 0.005 moles, concentration quenching was observed and the PL/PLE intensity was found to decrease with increasing doped Eu^{2+} content.

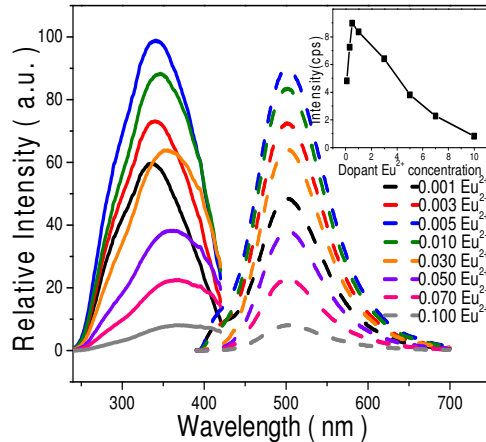


Fig. 3. Concentration dependence of relative PLE and PL intensity of CLP: $x\text{Eu}^{2+}$ ($x = 0.001 \sim 0.1$) under 365 nm excitation.

As indicated in Fig. 4(a), the Eu^{2+} emission of CLP: Eu^{2+} (solid line) at 400-600nm and centered at 502 nm (solid line) was assigned to the $4f^65d^1 \rightarrow 4f^7$ transition and the Mn^{2+} excitation of CLP: Mn^{2+} contains several bands centered at 267, 343, 370, 405, 417, and 454 nm (dash line), corresponding to the transitions from the ${}^6\text{A}_1({}^6\text{S})$ ground state to the excited states of ${}^4\text{T}_1({}^4\text{P})$, ${}^4\text{E}({}^4\text{D})$, ${}^4\text{T}_2({}^4\text{D})$, [${}^4\text{A}_1({}^4\text{G})$, ${}^4\text{E}({}^4\text{G})$], ${}^4\text{T}_2({}^4\text{G})$, and ${}^4\text{T}_1({}^4\text{G})$ levels, as reported by Ravikumar et al. [21]. We have observed a significant spectral overlap at around 454 nm between the Eu^{2+} PL and Mn^{2+} PLE spectra, which revealed that the spectral overlap is matched for Eu^{2+} and Mn^{2+} and a part of the energy can transfer from Eu^{2+} to Mn^{2+} . Therefore, there can be a good energy transfer from Eu^{2+} to Mn^{2+} in CLP: $\text{Eu}^{2+}, \text{Mn}^{2+}$ and an effective resonance-type energy transfer from Eu to Mn ($\text{ET}_{\text{Eu} \rightarrow \text{Mn}}$) was expected. Figure 4(b) shows the emission spectra of CLP: $0.005\text{Eu}^{2+}, x\text{Mn}^{2+}$ phosphors ($x = 0, 0.01, 0.015, 0.03, 0.05, 0.07$ and 0.1). For CLP: $0.005\text{Eu}^{2+}, x\text{Mn}^{2+}$ samples with $0.01 \leq x \leq 0.1$, two broad emission bands centered at 502 nm and 635 nm were observed, respectively. The emission band at 502 nm is viewed as the typical Eu^{2+} emission and the band at 635 nm is due to the Mn^{2+} emission. The PL intensity of Eu^{2+} at 502 nm was found to decrease with increasing Mn^{2+} content, and the PL intensity of Mn^{2+} at 635 nm increases with increasing Mn^{2+} content until the appearance of concentration quenching occurred at the sample with Mn^{2+} content of 0.07, which further supports the occurrence of the $\text{ET}_{\text{Eu} \rightarrow \text{Mn}}$ mechanism. Moreover, the observed variation of emission-tunable PL intensities of Eu^{2+} and Mn^{2+} in CLP: $0.005\text{Eu}^{2+}, x\text{Mn}^{2+}$ strongly support energy transfer from Eu^{2+} to Mn^{2+} .

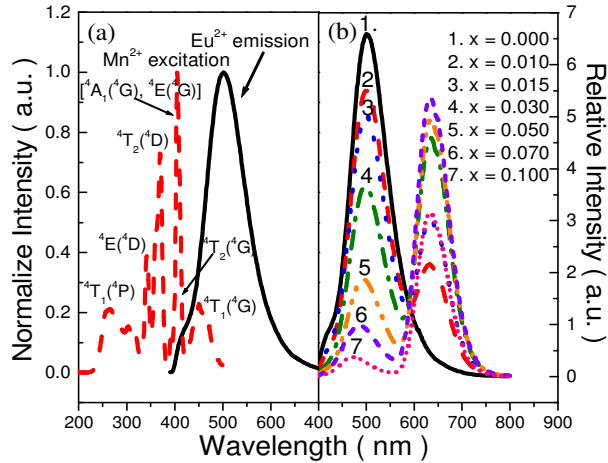


Fig. 4. (a) Spectral overlap between the Eu^{2+} PL spectrum of CLP:Eu^{2+} (solid line) and the PLE spectrum of CLP:Mn^{2+} (dash line); (b) The emission spectra of $\text{CLP:0.005Eu}^{2+}, x\text{Mn}^{2+}$ phosphors excited at 365 nm.

Table 1 reports the chemical compositions and the chromaticity coordinates of $\text{CLP:0.005Eu}^{2+}, x\text{Mn}^{2+}$ phosphors and Fig. 5 further represents the data in the 1931 CIE chromaticity diagram. The chromaticity coordinates of $\text{CLP:0.005Eu}^{2+}, x\text{Mn}^{2+}$ ranging from (0.282, 0.445) to (0.406, 0.388) and eventually to (0.637, 0.303), indicate that the color hue is tunable from green to yellow and, eventually, to red in the visible spectral region by changing the doped Mn^{2+} content. A white light with chromaticity coordinates (0.353, 0.324) was generated by a phosphor blend of a yellow-emitting $\text{CLP:0.005Eu}^{2+}, 0.015\text{Mn}^{2+}$ and a blue-emitting $\text{BaMgAl}_{10}\text{O}_{17}:\text{Eu}^{2+}$ (BAM:Eu^{2+}). For comparison, the YAG:Ce^{3+} with CIE chromaticity of (0.429, 0.553) pumped with an InGaN blue chip with chromaticity of (0.144, 0.030) can give white light with chromaticity of (0.291, 0.300) [22]. The inset of Fig. 5 shows three LEDs fabricated by pumping phosphors of CLP:0.005Eu^{2+} (photo 1), a mixture of $\text{CLP:0.005Eu}^{2+}, 0.015\text{Mn}^{2+}$ and blue BAM:Eu^{2+} (photo w), and $\text{CLP:0.005Eu}^{2+}, 0.1\text{Mn}^{2+}$ (point 7), respectively, with a 365 nm UV-chip under a forward bias of 350 mA.

Table 1. Comparison of CIE chromaticity coordinates for $\text{CLP:0.005Eu}^{2+}, x\text{Mn}^{2+}$ phosphors ($\lambda_{\text{ex}} = 365$ nm) and simulated white light using $\text{Y}_3\text{Al}_5\text{O}_{12}:\text{Ce}^{3+}$ phosphors ($\lambda_{\text{ex}} = 460$ nm).

Point No. in chromaticity diagram	Sample composition	(x, y)
1	$x = 0.000$	(0.281, 0.445)
2	$x = 0.010$	(0.367, 0.411)
3	$x = 0.015$	(0.406, 0.388)
4	$x = 0.030$	(0.495, 0.358)
5	$x = 0.050$	(0.573, 0.328)
6	$x = 0.070$	(0.620, 0.310)
7	$x = 0.100$	(0.637, 0.303)
w	$\text{CLP:0.005Eu}^{2+}, 0.015\text{Mn}^{2+} + \text{BAM:Eu}^{2+}$	(0.353, 0.324)
a	blue InGaN LED	(0.144, 0.030)
b	blue LED/ $\text{Y}_3\text{Al}_5\text{O}_{12}:\text{Ce}^{3+}$	(0.291, 0.300)
c	$\text{Y}_3\text{Al}_5\text{O}_{12}:\text{Ce}^{3+}$	(0.429, 0.553)

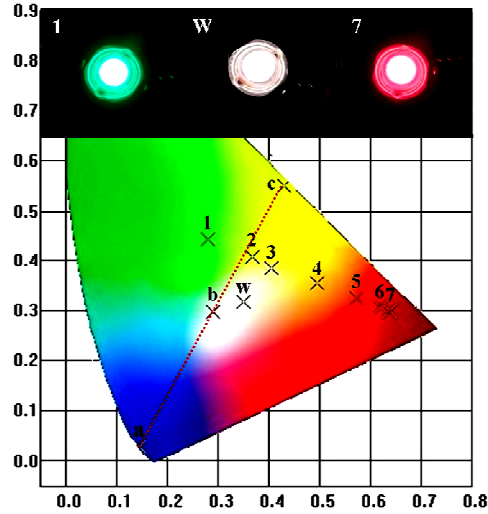


Fig. 5. CIE chromaticity diagram of $(\text{Ca}_{0.995-x})\text{La}(\text{PO}_4)_7:0.005\text{Eu}^{2+},x\text{Mn}^{2+}$ phosphors excited at 365 nm: x = (1) 0, (2) 0.01, (3) 0.015, (4) 0.03, (5) 0.05, (6) 0.07, and (7) 0.1.

The decay curves of $\text{CLP}:0.005\text{Eu}^{2+},x\text{Mn}^{2+}$ phosphors were measured and represented as shown in Fig. 6. The corresponding luminescence decay times can be best fitted with a second-order exponential decay mode (Fig. 6 dash line) by the following equation [23,24]:

$$I = A_1 \exp(-t / \tau_1) + A_2 \exp(-t / \tau_2) \quad (2)$$

where I is the luminescence intensity; A_1 and A_2 are constants; t is the time; and τ_1 and τ_2 are rapid and slow lifetimes for exponential components. Using these parameters, the average decay times (τ) can be determined by the formula given in the following [25]:

$$\langle \tau \rangle = (A_1 \tau_1^2 + A_2 \tau_2^2) / (A_1 \tau_1 + A_2 \tau_2) \quad (3)$$

The values of τ_1 , τ_2 , A_1 and A_2 are analyzed, determined, and summarized in Table 2, which indicates that in solely Eu^{2+} -activated system, the average decay time is long. However, in the $\text{Eu}^{2+}/\text{Mn}^{2+}$ co-doped system, the average decay time was found to be shortened with increasing doped Mn^{2+} content. Similar observations could be attributed to the formation of paired Mn^{2+} centers with faster decay than single Mn^{2+} centers, as proposed by Ruelle et al. [25] The average decay times (τ) were calculated to be 838, 768, 611, 424, 132, 55.7, and 25.8 ns for $\text{CLP}:0.005\text{Eu}^{2+},x\text{Mn}^{2+}$ with x = 0, 0.01, 0.015, 0.03, 0.05, 0.07, and 0.1, respectively. The inset of Fig. 6 clearly shows the relation between energy transfer efficiency (η_T) and concentration of Mn^{2+} ions. The η_T from Eu^{2+} to Mn^{2+} can be expressed according to Paulose et al. [26]

$$\eta_T = 1 - \frac{\tau_s}{\tau_{s0}} \quad (4)$$

where τ_s is the lifetime of Eu^{2+} in the presence of Mn^{2+} and τ_{s0} is the lifetime of the sensitizer Eu^{2+} in the sample in the absence of Mn^{2+} . The η_T was determined to be 0%, 18.2%, 41.9%, 59.7%, 81.1%, 89.8% and 95.6% for $\text{CLP}:0.005\text{Eu}^{2+},x\text{Mn}^{2+}$ with x = 0, 0.01, 0.015, 0.03, 0.05, 0.07, and 0.1, respectively. These results indicate that the η_T of $\text{CLP}:0.005\text{Eu}^{2+},x\text{Mn}^{2+}$ increases with increasing Mn^{2+} dopant content.

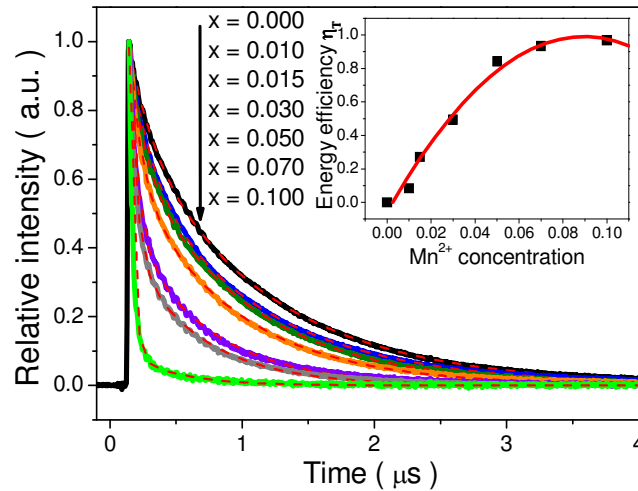


Fig. 6. Decay curves of Eu^{2+} emission for $\text{CLP:0.005Eu}^{2+},x\text{Mn}^{2+}$ (solid line) monitored at 502 nm and dash line indicates fitted curves. The inset shows the correlation between η_T and x under 365nm excitation.

Table 2. Decay times of $\text{CLP:0.005Eu}^{2+},x\text{Mn}^{2+}$ phosphors excited at 365 nm with emission monitored at 502 nm.

Samples	τ_1	A_1	τ_2	A_2	τ (ns)
$x = 0.000$	1.79E-7	0.74	9.62E-7	0.73	838
$x = 0.010$	1.52E-7	0.75	8.78E-7	0.73	768
$x = 0.015$	9.12E-8	1.89	7.76E-7	0.70	611
$x = 0.030$	6.57E-8	4.06	6.60E-7	0.61	424
$x = 0.050$	4.19E-8	18.65	4.54E-7	0.48	132
$x = 0.070$	3.49E-8	45.50	3.57E-7	0.31	55.7
$x = 0.100$	2.57E-8	118.38	2.58E-8	118.21	25.8

Based on Dexter's energy transfer formula of multi-polar interaction and Reisfeld's approximation, the following relation can be obtained [27,28]:

$$\frac{\tau_{s0}}{\tau_s} \propto C^{\alpha/3} \quad (5)$$

where C is Mn^{2+} ions concentration. As $(\tau_{s0}/\tau_s) \propto C^{\alpha/3}$ with $\alpha = 6, 8,$ and 10 corresponds to dipole-dipole, dipole-quadrupole, and quadrupole-quadrupole interaction, respectively. The relationship of $(\tau_{s0}/\tau_s) \propto C^{\alpha/3}$ was illustrated in Fig. 7 and a linear behavior was observed only when $\alpha = 8$, so that energy absorbed by Eu^{2+} is transferred to Mn^{2+} by a nonradiative dipole-quadrupole mechanism. The above results indicate that energy transfer occurs between Eu^{2+} and Mn^{2+} in $\text{CLP:Eu}^{2+},x\text{Mn}^{2+}$ phosphor and the relative intensity of green and red emission could be tuned by adjusting the relative concentration of Eu^{2+} and Mn^{2+} , respectively.

According to dipole-quadrupole mechanism, the critical distance of energy transfer from a sensitizer Eu^{2+} to an activator Mn^{2+} is given by:

$$P_{Eu-Mn}^{DQ} = 0.63 \times 10^{28} \frac{f_q \lambda_s^2 Q_a}{\tau_{s0} R_{Eu-Mn}^8 f_d E_s^4} \int F_s(E) F_a(E) dE \quad (6)$$

where $Q_a = 4.8 \times 10^{-16}$ and f_d is the absorption coefficient of Mn^{2+} ; $f_d = 10^{-7}$ and $f_q = 10^{-10}$ are the oscillator strengths of dipole and quadrupole electrical absorption transitions for Mn^{2+} ; λ_s (Å) and E (eV) are the emission wavelength and emission energy of Eu^{2+} , and $\int F_s(E) F_a(E) dE$ represents the spectral overlap between the Eu^{2+} and Mn^{2+} and it was estimated be $1.3565eV^{-1}$ [29]. The critical distance R_c of energy transfer from Eu^{2+} to Mn^{2+} is defined as the distance for which the probability of transfer equals the probability of radiative emission of Eu^{2+} , i.e., the distance for which $P_{Eu-Mn}^{DQ} \tau_{s0} = 1$. Therefore, R_c can be calculated using the following equation [29,30]:

$$R_c^8 = 0.63 \times 10^{28} \frac{f_q \lambda_s^2 Q_a}{f_d E_s^4} \int F_s(E) F_a(E) dE \quad (7)$$

In this system, the critical distance of energy transfer in $CLP:Eu^{2+}, Mn^{2+}$ phosphor was calculated to be about 11.36 Å, which is similar to those obtained for $Ca_2MgSi_2O_7:Eu^{2+}/Mn^{2+}$ (11.97 Å) [7] and $Sr_2Zn(PO_4)_2:Eu^{2+}/Mn^{2+}$ (11.4 Å) [10].

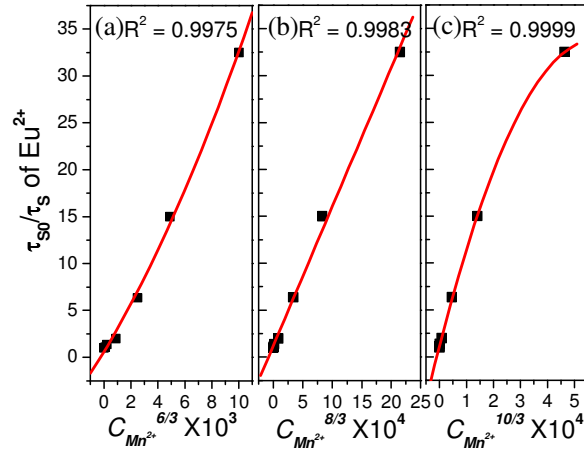


Fig. 7. Dependence of τ_{s0}/τ_s of Eu^{2+} on (a) $C^{6/3}$, (b) $C^{8/3}$ and (c) $C^{10/3}$.

Figure 8 shows the PL spectra of $CLP:0.005Eu^{2+}, 0.015Mn^{2+}$ (black line), $BAM:Eu^{2+}$ commodity (blue line) and a blend of yellow $CLP:0.005Eu^{2+}, 0.015Mn^{2+}$ and blue-emitting $BAM:Eu^{2+}$ (dash line) commodity pumped with a UV-LED chip (365 nm). Shown in Fig. 9 is the EL spectrum of a white LED lamp fabricated with the above-stated phosphor blend and silicon resin pumped with a 365 nm UV-LED chip and driven with a 350-mA current. The white light generated shows CIE color coordinates (0.35,0.31) and Ra of 91.5, as determined from the full set of the 8 CRIs average Ra values shown in Table 3. The upper-right inset of Fig. 9 shows the appearance of a phosphor-converted LED lamp under a forward bias of 350 mA. These results demonstrated that our phosphor blend ($CLP:Eu, Mn$ and $BAM:Eu^{2+}$)-converted white-light UV-LED shows higher Ra value (91.5) and lower CCT (4,496K) than those (i.e., $Ra = 75$, CCT = 7756K) of a white LED fabricated with $YAG:Ce^{3+}$ phosphor pumped with blue InGaN chip [1].

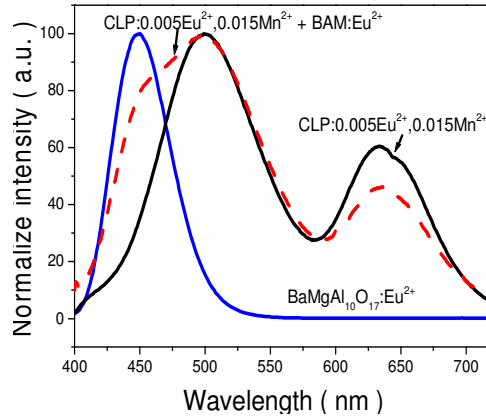


Fig. 8. The PL spectrum of $(\text{Ca}_{0.98})_9\text{La}(\text{PO}_4)_7:0.005\text{Eu}^{2+},0.015\text{Mn}^{2+}$, $\text{BaMgAl}_{10}\text{O}_{17}:\text{Eu}^{2+}$ and the white-emitting phosphors of a mixture of $(\text{Ca}_{0.98})_9\text{La}(\text{PO}_4)_7:0.005\text{Eu}^{2+},0.015\text{Mn}^{2+}$ and $\text{BaMgAl}_{10}\text{O}_{17}:\text{Eu}^{2+}$.

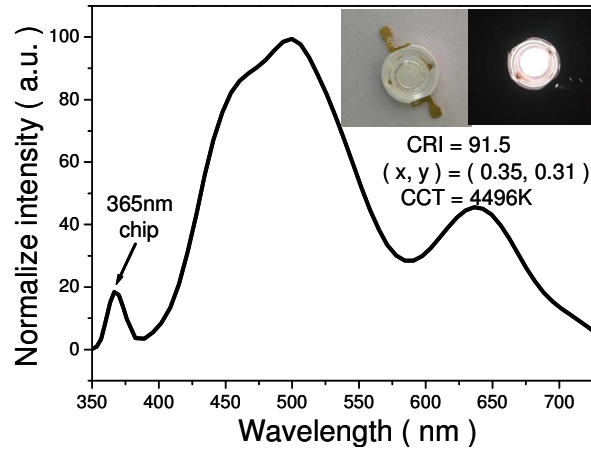


Fig. 9. EL spectrum of a white LED lamp fabricated using a UV-chip (365 nm) and a phosphor blend of $(\text{Ca}_{0.98})_9\text{La}(\text{PO}_4)_7:0.005\text{Eu}^{2+},0.015\text{Mn}^{2+}$ and $\text{BaMgAl}_{10}\text{O}_{17}:\text{Eu}^{2+}$ under a forward bias of 350 mA.

Table 3. Full set of the 8 CRIs and the Ra values of $(\text{Ca}_{0.98})_9\text{La}(\text{PO}_4)_7:0.005\text{Eu}^{2+},0.015\text{Mn}^{2+}$ and $\text{BAM}:\text{Eu}^{2+}$ with a 365 nm UV-LED

R1	R2	R3	R4	R5	R6	R7	R8	Ra
96	91	86	93	95	88	89	94	91.5

4. Conclusion

In conclusion, a series of single-composition emission-tunable CLP: $\text{Eu}^{2+},\text{Mn}^{2+}$ phosphors were synthesized and investigated. The energy transfer from sensitizer Eu^{2+} to activator Mn^{2+} in $\text{Ca}_9\text{La}(\text{PO}_4)_7$ host has been studied and demonstrated to be a resonant type via a dipole-quadrupole mechanism based on the decay lifetime data and the energy transfer critical distance was estimated to be 11.36 Å by using the spectral overlap method. We have improved the Ra and reduced CCT value of white LEDs by using a phosphor blend of yellow-emitting $\text{Ca}_9\text{La}(\text{PO}_4)_7:0.005\text{Eu}^{2+},0.015\text{Mn}^{2+}$ and blue-emitting $\text{BaMgAl}_{10}\text{O}_{17}:\text{Eu}^{2+}$ commodity pumped with UV-LED chip (365 nm). Our investigation results indicate that the warm white-

emitting UV-LED based on phosphor blend of CLP:Eu,Mn and BAM:Eu²⁺ exhibits superior *Ra* and CCT to those of conventional white LED based on YAG:Ce³⁺ pumped with blue LED chips.

Acknowledgments

This research was supported by National Science Council of Taiwan (ROC) under contract No. NSC98-2113-M-009-005-MY3 (T.-M. C.) and, in part, by Industrial Technology Research Institute under contract No. 7301XS1861 (C.-H. H.).